

Biliary cirrhosis-induced cardiac abnormality in rats: Interaction between Farnesoid-X-activated receptors and the cardiac uncoupling proteins 2 and 3

Gholamreza Bayat^{1, 2}, Seyed Ali Hashemi³, Hosein Karim^{2, 4}, Parviz Fallah⁵, Keshvad Hedayatyanfard^{1, 2}, Mahnaz Bayat⁶, Azadeh Khalili^{1, 2*}

¹ Department of Physiology-Pharmacology-Medical Physic, School of Medicine, Alborz University of Medical Sciences, Karaj, Iran

² Cardiovascular Research Center, Alborz University of Medical Sciences, Karaj, Iran

³ Department of Pathology, School of Medicine, Alborz University of Medical Sciences, Karaj, Iran

⁴ Department of Cardiology, School of Medicine, Alborz University of Medical Sciences, Karaj, Iran

⁵ Department of Medical Laboratory Sciences, Faculty of Para-Medicine, Alborz University of Medical Sciences, Karaj, Iran

⁶ Clinical Neurology Research Center, Shiraz University of Medical Sciences, Shiraz, Iran

ARTICLE INFO

Article type:

Original

Article history:

Received: Oct 10, 2022

Accepted: Jan 3, 2022

Keywords:

Cardiomyopathy

Cholestasis

Farnesoid-X-receptor

Liver cirrhosis

Mitochondrial uncoupling - proteins

ABSTRACT

Objective(s): This study aimed to evaluate the relationship between Farnesoid-X-activated receptors (FXR) as nuclear regulators of the antioxidant defense system as well as cardiac mitochondrial carrier proteins of UCP2 and UCP3 in cardiac damage induced by cirrhosis.

Materials and Methods: Twenty-two male Wistar rats (200–250 g) were randomly divided into 3 experimental groups, including a control group (n=6), a sham-operated group (n=8), and a bile duct ligated (BDL) group (n=8). Four weeks after surgical intervention, biochemical assessment (AST, ALT, GGT, LDH, and ALP), histological observation, and molecular evaluation (FXR, UCP2, UCP3, BNP, Caspase3, and GAPDH) using real-time RT-PCR were performed.

Results: Compared with the sham-operation group, the BDL group showed a significant rise in liver enzymes of AST, ALT, GGT, LDH, and ALP. Defined fibrotic and necrotic bundles and thick reticulin fibers were also found in BDL liver tissue. Besides liver morphological alterations, left ventricles of BDL ones were also associated with defined cardiomyocyte hypertrophy, myofiber vacuolization, and clear pigmentation. Findings showed a significant up-regulation of cardiac Brain Natriuretic Peptide (BNP) along with marked down-regulation in hepatic FXR, cardiac FXR, and cardiac UCP2 and UCP3. However, the expression of caspase 3 in the cardiac tissue was not affected by BDL operation during 4 weeks.

Conclusion: Expression of FXR as an upstream regulator of cellular redox status, besides the non-enzymatic ROS buffering defense system of cardiac UCPs, has a pivotal role in the pathogenesis of cirrhotic-induced cardiac abnormality in rats.

► Please cite this article as:

Bayat GhR, Hashemi SA, Karim H, Fallah P, Hedayatyanfard K, Bayat M, Khalili A. Biliary cirrhosis-induced cardiac abnormality in rats: Interaction between Farnesoid-X-activated receptors and the cardiac uncoupling proteins 2 and 3. Iran J Basic Med Sci 2022; 25:126-133. doi: <https://dx.doi.org/10.22038/IJBMS.2022.60888.13485>

Introduction

Cirrhosis is a progressive liver disease that could negatively affect cardiac function. The term “cirrhotic cardiomyopathy” was first introduced to explain the manifestation of cardiac dysfunction in cirrhotic patients who did not suffer from the previous cardiac disease (1). The spectrum of this cardiac abnormality is started from an early diastolic dysfunction seen to some degree in all patients (2). It could be extended into the late systolic dysfunction, which appears only in stress conditions (3). Although the precise leading mechanisms of this second type of cardiac dysfunction are not fully determined, several underlying mechanisms have been suggested to participate in the development and progression of these structural and functional abnormalities. One of the most crucial underlying mechanisms is a chronic and dramatic change in the redox state. Cellular redox status progressively changes toward the production of pro-oxidant markers and suppression of the

antioxidant defense system in liver disease (4). Impairment of cellular mitochondrial function and energy metabolism, which strongly facilitate reactive oxygen species (ROS) formation (5, 6), are also associated with cirrhosis-induced cardiac dysfunction (7).

Uncoupling proteins (UCPs) that effectively adjust mitochondrial ROS generation are located in the mitochondrial inner membrane. They reduced mitochondrial ROS production by inducing proton leak and decreased proton gradient across the mitochondrial inner membrane (8). So, UCPs serve as a non-enzymatic cellular antioxidant system that reduces ROS generation at oxidative stress conditions (9). UCP2 and UCP3 are members of the UCPs superfamily, which are predominantly expressed in the myocardium. Several experimental studies indicate that cardiac UCPs expression could be influenced by disease status. As reported by Bugger *et al.*, doxorubicin-induced heart failure was associated with a significant

*Corresponding author: Azadeh Khalili. Department of Physiology-Pharmacology-Medical Physic, School of Medicine, Alborz University of Medical Sciences, Karaj, Iran. Tel: +98-26-34287425; Fax: +98-26-34287425; Email: a.khalili@abzums.ac.ir

down-regulation of myocardial UCP2 and UCP3, which could potentiate ROS generation and produce more cardiac damage (10). Other previous studies have also obtained similar results. The Overexpressed-UCP1 heart was effectively protected from ischemia/reperfusion injury and oxidative damage in transgenic mice (11). Over-expression of UCP2 in neonatal cardiomyocytes exposed to hydrogen peroxide also behaved as a cardioprotective factor and remarkably reduced cell markers of apoptosis (12).

Cellular redox hemostasis is also controlled by the upstream regulatory sites of the gene via some specific ligand-activated nuclear transcription factors. Farnesoid-X-activated receptors (FXR) are members of the nuclear receptor superfamily, which have a central role in bile acid, lipid, and cholesterol metabolism. FXR is considered an upstream controller of the cellular redox state, apart from its role in metabolic pathways. The mentioned regulatory role is mediated via activation of several upstream and downstream signaling pathways such as activation of transcriptional factor NrF2, and as a consequence increasing the formation of cellular glutathione (GSH), superoxide dismutase (SOD), and several other endogenous antioxidants (13-15). Therefore, activation of FXR and FXR target genes play an essential role in modulating the deleterious effects of free radicals in pathological conditions (13, 16, 17). The role of cardiac FXR activation has been investigated in several recent studies. Both cardioprotective (18, 19) and cardiosuppressive (20) effects have been attributed to this type of nuclear receptor. FXR is also contributed as a regulatory part in cytoprotection, anti-inflammatory, and anti-apoptotic program. These activities of the FXR are closely related to its regulatory effects on mitochondrial function (21).

Acknowledging the crucial role of mitochondria in energy supply and ROS production and considering the regulatory effect of FXR on the key mitochondrial signaling pathways, the present study aimed to evaluate the relationship between changes in cardiac expression of FXR, UCP2, and UCP3 in a rat model of cirrhosis. The correlation between cardiac and hepatic mRNA levels of FXR was also investigated. In the present study, the induction of biliary cirrhosis via bile duct ligation was considered as an experimental model for secondary cardiac abnormality.

Materials and Methods

Ethical approval

All experiment procedures were carried out according to the international conventions on animal experimentation and approved by the institutional ethics committee of Alborz University of Medical Sciences (IR.ABZUMS.REC.1397.037). Also, this study complies with the ethical principles under which experimental physiology operates.

Chemicals

Ketamine and xylazine were obtained from Alfasan (Woerden, Holland).

Animals

Twenty-two eight-week-old male Wistar rats weighing 200–250 g were kept in standard conditions, including controlled room temperature (22±2 °C) with a 12 hr:12 hr light/dark cycle and relative humidity of 40%-50%. During the study, animals had free access to food and water.

Experimental design and protocol

Animals were randomly divided into 3 experimental

groups, including a control group (n=6), a sham-operated group (n=8), and a bile duct ligation (BDL) group (n=8). The surgical procedure was performed in clean conditions. Animals were anesthetized using a single intraperitoneal injection of ketamine (60 mg/kg) and xylazine (8 mg/kg). After diminution of the animals' reflexes, ligation of the bile duct was performed according to the methods described by Yang *et al.* (22). Briefly, after middle line incision and cleaning the surrounding tissue, the bile duct was tightly double-ligated using 4-0 silk sutures, first near the junction of the hepatic ducts, and the second was made above the entrance of the pancreatic duct. Then the middle site between the ligatures was transected. The Sham-operated group underwent all surgical procedures without ligation. The abdominal wall and skin incisions were then sutured using absorbable (3-0 catgut) and non-absorbable (3-0 silk) suture materials, respectively. After that, animals were transferred into separate cages. The wounds were kept clean for the first week of the procedure with topical tetracycline ointment (Tetracycline-najo 3%, Iran-Najo. co). The duration of the experiment was 4 weeks.

Biochemical analysis

On the 28th day of the experiment, all animals were anesthetized with an intraperitoneal injection of ketamine (60 mg/kg) and xylazine (8 mg/kg). Under deep anesthesia, thoracotomy was performed, and blood samples were gently collected from the heart. To evaluate the liver function, serum levels of aspartate aminotransferase (AST), alanine aminotransferase (ALT), lactate dehydrogenase (LDH), gamma-glutamyltransferase (GGT), and alkaline phosphatase (ALP) were measured (23) using commercial kits (Pars Azmun Co, INC, Karaj, Iran) according to the manufacturer's guidelines.

Heart and body weights

After collecting blood samples, the hearts were isolated and weighed. For a logical interpretation, the animal's absolute heart weight was normalized to body weight (HW/BW).

Histopathological examination

Animals' livers and hearts were dissected out and prepared for histopathological studies. Therefore, the most prominent right lobe of each liver and the left ventricle were cut and immediately fixed in a 10% formalin solution. Tissue staining of Hematoxylin and Eosin (H&E), Masson's Trichrome, and Reticulin was performed to detect any pathological signs of injury, fibrotic scars, or necrotic lesion of the liver, respectively. Cardiac samples were also evaluated using H&E and Masson's trichrome staining.

Real time-RT PCR assessment

Real-time RT PCR was performed to identify the quantitative level of mRNA for our targeted genes of FXR, UCP2, UCP3, Caspase 3, and BNP according to the protocol (24). Briefly, 50 mg of either the left ventricle or liver tissue was homogenized using a polytron tissue homogenizer (DAIHAN-brand Homogenizing Stirrer, HS-30E; Korea). The RNA was then extracted using Trizol (Qiagen) based on the manufacturer's instructions. Then cDNA synthesis was performed using a reverse transcriptase cDNA synthesis kit (Fermentas), based on the protocol. Expression of the aforementioned genes was measured by Real-Time

Table 1. Forward and reverse sequence of all primers used in the present study

Target gene	Foreword sequence	Reverse sequence
FXR	TGGGAATGTTGGCTGAATG	CCTGTGGCATTCTCTGTTTG
UCP2	CCTGTGTTCTCCTGTGTATTG	CTTCTCTAAAGGTGTCCCG
UCP3	CGAGAGGAAATACAGAGGGAC	GGGAAGTTGTCAGTGAACAG
BNP	GCTCCTGCTTTTCCTTAATCTG	GCCATTTCTCTGACTTTTCTC
Caspase3	GCTTACTCTACCGCACCC	GCGTACAGTTTCAGCATGG
GAPDH	GCCTTCTCTGTGACAAAGTG	CTTCCCATTCTCAGCCTTG

FXR: Farnesoid-X-activated Receptor, UCP: Uncoupling Protein, BNP: Brain Natriuretic Peptide

Table 2. Serum levels (mean ± SEM, n = 8) of aspartate aminotransferase (AST), alanine aminotransferase (ALT), lactate dehydrogenase (LDH), gamma-glutamyltransferase (GGT), and alkaline phosphatase (ALP) in the experimental groups including the Control group (n=6), Sham-operated group (n=8), and Bile duct ligation group (BDL, n=8) after 4 weeks

	AST	ALT	LDH	GGT	ALP
Control	139.4±7.7	106.0±5.7	296.7±28.1	6.0±1.1	880.0±78.5
Sham	127.8±13.2	115.8±5.4	334.0±32.2	7.4±1.36	857.7±60.0
BDL	447.5±23.1***	184.3±14.6***	466.0±38.2*	58.0±13.6**	1696.4±109.3***

*Significant difference from the control group (*P≤ 0.05, ** P≤ 0.01, *** P≤ 0.001)

PCR using SYBR GREEN (TAKARA). Experiments were performed in duplicates as follows: denaturation at 95 °C for 10 min subsequently followed by 45 cycles at 95 °C for 10 sec, 60 °C for 10 sec, and 72 °C for 10 sec. The expression level was normalized to the GAPDH and expressed as fold-change. The exact nucleotide sequences of the genes and GAPDH primers are shown in Table 1.

Statistical analysis

Data were expressed as mean±SEM. One-way analysis of variance (ANOVA) was conducted for between-group analysis. Duncan’s multiple range test was a *post hoc* test to measure specific differences between pairs of means. A P-value of less than 0.05 was considered statistically significant. Graphpad Prism 8 (8.0.2) software was applied for data analysis and creating graphs.

Results

Effects of bile duct ligation on liver function

As summarized in Table 2, there were no significant differences between the control and sham groups for all biochemical enzymes. In contrast, the serum levels of AST (P<0.001), ALT (P<0.001), LDH (P=0.038), GGT (P=0.010), and ALP (P<0.001) were significantly increased in the BDL group compared with the sham-operated group.

Effects of bile duct ligation on HW and HW/BW ratio

Body weights, absolute and the normalized heart weights

Table 3. Values (mean ± SEM) of Body weight (BW), Absolute heart weight (HW), and Heart weight/body weight ratio (HW/BW) in the experimental groups including the Control group (n=6), Sham-operated group (n=8), and Bile duct ligation group (BDL, n=8) after 4 weeks

	BW (G)	ABSOLUTE HW (MG)	HW/BW (MG/G)
CONTROL	278.4±5.06	1048.6±27.0	3.76±0.11
SHAM	268.2±2.31	1031.2±9.3	3.84±0.05
BDL	289.5±13.0	1293.6±27.2***	4.47±0.09**

*Denotes significant difference (**P≤ 0.01, *** P≤ 0.001)

were presented in Table 3. The sham operation did not associate with any significant changes in the absolute and normalized heart weights. However, 4 weeks ligation of the bile duct significantly increased either absolute HW (P<0.001) or HW/BW ratio (P=0.002).

Effects of bile duct ligation on histopathological changes of liver and heart

Changes in the liver histology have been shown in Figure 1 and Table 4. Although the sham operation did not affect tissue structure and histology (Figures 1d, e, f), bile duct ligation led to a significant disarrangement in

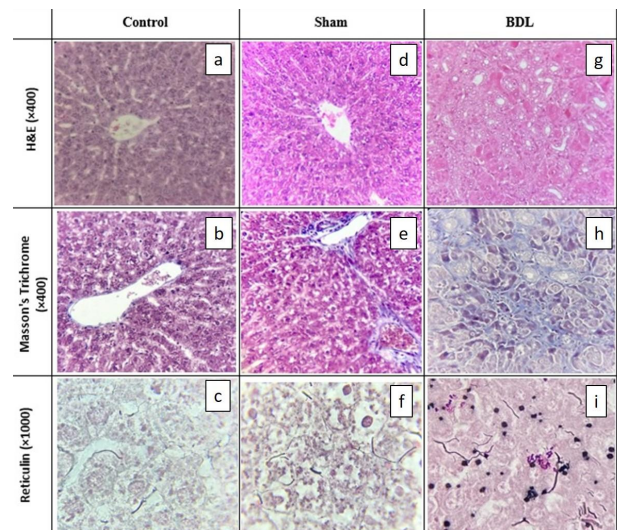


Figure 1. Longitudinal section of hepatic tissue stained by H&E, Masson’s trichrome, and Reticulin. Compared with H&E staining of the control (a) and sham groups (d), bile duct ligation (g) was associated with a significant disarrangement in liver architecture. Obvious proliferation of the bile duct along with clear focal inflammation and necrosis were detected (g). Masson’s trichrome (h) and reticulin (i) staining showed the development of well-defined fibrotic bundles and noted thickening of reticulin fibers induced by BDL, respectively

Table 4. Comparison of histological injuries evaluated by three staining methods in experimental groups including the Sham-operated group, Bile duct ligation (BDL) group, and BDL group for 28 days. Data were presented as median

Groups		Control	Sham	BDL
Liver histology: H&E staining				
1	Glycogen depletion	0	0	3**
3	Congestion	0	0	0
4	Sinusoidal dilation	0	0	2.5**
5	Inflammatory infiltration	0	0	2.5**
6	Plasma cells	0	0	1*
7	Bile duct proliferation	0	0	3**
8	Kupffer cell hyperplasia	0	0	3**
9	Pyknosis	0	0	1.5*
10	Karyolysis/Apoptosis	0	0	1.5*
11	Regeneration	0	0	2.5**
Liver histology: Mason's trichrome staining				
	Fibrotic bundles	0	0	2**
Liver histology: Reticulin staining				
	Necrosis	0	0	2.5**

0: no abnormality detected; 1: damage/active changes up to 25%; 2: damage/active changes up to 50%; 3: damage/active changes up to 75%; 4: damage/active changes >75%

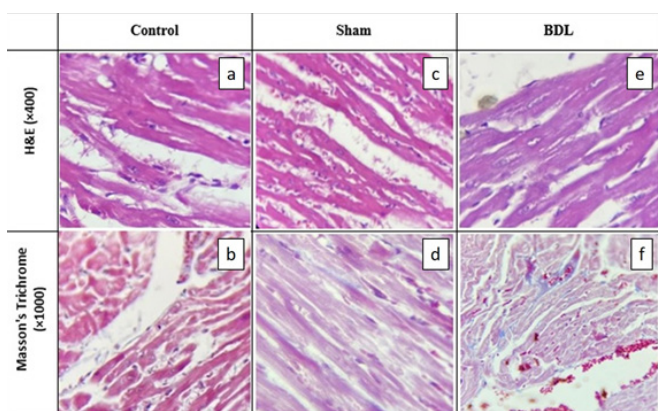


Figure 2. Longitudinal section of cardiac tissue stained by H&E and Masson's trichrome. Compared with H&E staining of control (a), and sham groups (c), bile duct ligation (e) was associated with cardiomyocyte hypertrophy, myofiber vacuolization, and changed pigmentation. An increase in the number of inter-cardiac fibroblasts, nuclei enlargement, and infiltration of the inflammatory cells was induced by 4-week ligation of the bile duct (e). Masson's trichrome staining showed mild fibrosis in the BDL-cardiac section (f)

liver architecture (Figures 1g, h, i). Assessment of the liver histology using H&E determined a significant infiltration of

inflammatory cells along with evident sinusoidal dilation, bile duct proliferation, Kupffer cell hyperplasia, and obvious signs of regeneration (Table 4). In addition, the development of apoptosis, fibrosis, and necrosis was also found in the H&E staining of liver samples. Masson's trichrome and reticulin staining of the liver samples also confirmed the development of fibrotic and thickening of reticulin fiber, respectively (Table 4).

Alteration of the cardiac tissue following bile duct ligation has been shown in Figure 2 and Table 5. Compared with the control group, H&E cardiac tissue staining in the BDL group showed cardiomyocyte hypertrophy, myofiber vacuolization, and changed pigmentation in the BDL group. The number of fibroblasts was also increased between cardiac muscle fibers. Nuclei enlargement, internalization, and inflammatory cell infiltration were other signs of histopathological changes induced by bile duct ligation during 28 days (Figure 2e, Table 5). Specific evaluation of fibrosis in cardiac tissue using Masson's trichrome staining showed mild fibrosis in BDL-cardiac samples (Figure 2f, Table 5).

Effects of bile duct ligation on gene expression change in the heart and liver

Changes in the gene expression induced by BDL have been shown in Figure 3. There were no significant differences between the sham and control groups in this

Table 5. Comparison of histological injuries evaluated by three staining methods in experimental groups including the Sham-operated group, Bile duct ligation (BDL) group, and BDL group for 28 days. Data were presented as median

Groups		Control	Sham	BDL
Cardiac histology: H&E staining				
1	Cardiomyocyte hypertrophy	0	0	1*
2	Altered pigmentation	0	0	1**
3	Number of fibroblasts between the cardiac muscle fibers	0	0	1*
4	Disorganized cardiac muscle fiber	0	0	0
5	Myofiber vacuolization	0	0	1*
7	Cell infiltration	0	0	1**
8	Enlargement/internalization of nuclei			1*
Cardiac histology: Mason's trichrome staining				
	Fibrotic bundles	0	0	0.5

0: no abnormality detected; 1: damage/active changes up to 25%; 2: damage/active changes up to 50%; 3: damage/active changes up to 75%; 4: damage/active changes >75%

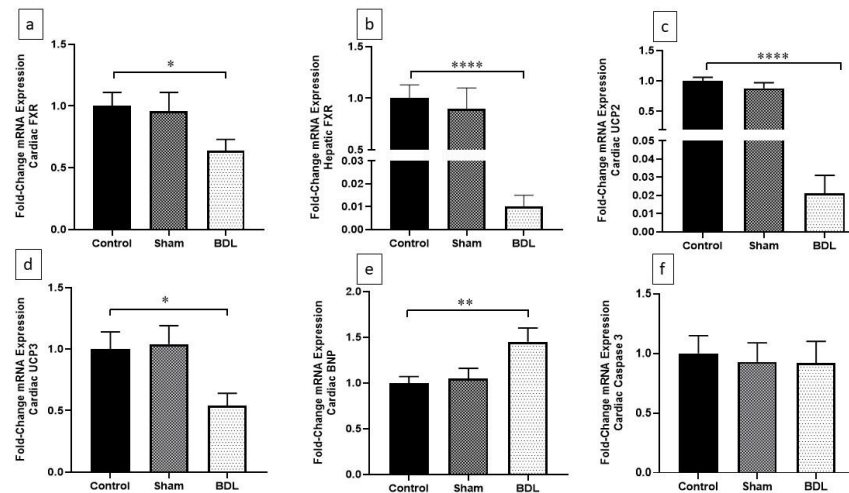


Figure 3. Effect of Bile duct ligation (BDL) on the expression of (a) cardiac Farnesoid-X-activated receptors (FXR), (b) hepatic FXR, (c) cardiac uncoupling protein 2 (UCP2), (d) cardiac uncoupling protein 3 (UCP3), (e) cardiac brain natriuretic peptide (BNP), and (f) cardiac caspase 3 genes in the experimental groups (n=8) including control, sham, and Bile duct ligation (BDL) groups. Data were expressed as mean±SEM. * $P<0.05$; ** $P<0.01$; *** and $P<0.001$

regard. However, ligation of the bile duct for 4 weeks was associated with significant changes in the expression of targeted genes of both cardiac and hepatic tissue. As shown in Figure 3a, in the BDL group, cardiac expression of the FXR gene was significantly reduced compared with the control one (0.645 vs 1.0; $P=0.017$). Inconsistent with cardiac FXR mRNA level, the expression of hepatic FXR (Figure 3b) was also significantly decreased in the BDL group (0.015 vs 1.0; $P<0.001$). As shown in Figures 3c and d, cardiac UCP2 (0.02 vs 1.0, $P=0.001$) and UCP3 (0.54 vs 1.0, $P=0.02$) were also significantly down-regulated following 4-week ligation of the bile duct. In contrast, the mRNA level of cardiac BNP (1.41 vs 1.0, $P=0.003$) was significantly increased in the BDL one (Figure 3e). Despite the development of these significant changes in the expression of cardiac and hepatic genes, the mRNA level of cardiac caspase 3 was not associated with any significant difference compared with the control group.

Discussion

The present study was designed to mechanistically evaluate the role of cardiac FXR, UCP2, and UCP3 in the secondary cardiac abnormality due to biliary cirrhosis. It also aimed to understand the correlation between the expression of cardiac and hepatic FXR and the relationship between alteration of cardiac FXR expression and cardiac UCPs. Besides the development of dark-yellow urine, yellow discoloration of the skin, and late ascites, induction of severe liver damage was also confirmed by biochemical and histopathological findings. Significant elevation of AST, ALT, LDH, GGT, and ALP and histological alterations, including the development of fibrotic and necrotic bundles, were considered liver damage manifestations. Hepatic dysfunction resulted in the development of secondary cardiac abnormality characterized by cardiac hypertrophy. The latter was confirmed by cardiac histopathological signs, elevated absolute HW and HW/BW ratio, and significant up-regulation of cardiac BNP. Besides these apparent signs of liver and heart damages, alterations in targeted genes expressed in both tissues were also found. Our findings indicated that down-regulation of cardiac FXR was consistent with that of its hepatic expression. Following

the hepatic FXR, cardiac FXR, UCP2, and UCP3 were also down-regulated following 4-weeks of bile duct ligation. However, changes in myocardial mRNA level of caspase 3 were not found following 4-week ligation of the bile duct.

Cirrhotic cardiomyopathy occurred in about 50% of cirrhosis cases (25). It was primarily introduced as one of the systemic manifestations of cirrhosis independent of etiology. Disease manifestations range from a mild diastolic dysfunction at early stages to late systolic dysfunction in stress conditions (2, 3). Despite various studies on liver damage due to biliary obstruction, few reports deal with secondary cardiac abnormality induced by BDL. According to a study, 4-week ligation of bile duct resulted in morphological, functional, and molecular abnormalities in cardiac tissue manifested by massive atrial fibrosis, weak chronotropic responsiveness to isoproterenol, and over-expression of transforming growth factor β (TGF- β), respectively (26). Other cardiac abnormalities induced by biliary obstruction have also been reported. The imbalanced proportion of oxidative to antioxidative markers, including an elevated level of malondialdehyde (MDA) along with decreased amount of some antioxidant enzymes such as glutathione, catalase, and superoxide dismutase (SOD), was also shown in cardiac tissue of cholestatic animals (27). In addition, BDL-induced hepatic cardiomyopathy was associated with activation of liver-heart inflammatory pathways and marked hemodynamic impairment, including systolic, diastolic, and macrovascular dysfunction in BDL animals (28). Depressed cellular respiration of the heart due to reduced cardiac mitochondrial capacity was also exhibited in BDL rats (29). Our findings are consistent with previous ones, which exhibited the development of secondary cardiac complications due to biliary obstruction. Left ventricles of BDL hearts were associated with evident cardiomyocyte hypertrophy, myofiber vacuolization, and altered pigmentation. According to previous findings, these cardiac morphological alterations could represent signs of diastolic dysfunction which in the case of the present study is induced by biliary obstruction (30, 31). Besides morphological changes, cardiac hypertrophy is also confirmed by a significant increase in either absolute or

normalized HW as well as obvious up-regulation of BNP. BNP is an early predictor of cardiac disability (32). There are several reports (32, 33) that indicate the overexpression of BNP in primary or secondary cardiac disease. Elevated serum levels of natriuretic peptides (NPs) such as ANP, BNP, or their fragments such as MR-proANP and NT-proBNP represent ventricular wall stress and are interpreted as development of cardiac hypertrophy and/or mild to severe degree of heart failure (34). According to preclinical and clinical studies, increased serum level and/or mRNA expression of NPs is associated with a wide spectrum of cardiac complications including ischemic heart disease, valvular and rhythm abnormality, contractility, filling pressure dysfunction, and congenital heart disease (34). Despite conducting several basic investigations to shed light on the mechanisms involved in the cirrhotic-induced cardiac abnormality, many aspects of its pathogenesis remain unknown.

Mitochondria act as cellular sources of energy and ROS generation in physiologic conditions. Mitochondria are also critical regulators of cellular apoptosis program and cytosolic calcium ion balance (35). In the heart, mitochondria maintain energy supply to provide sufficient fuel for effective myocardial excitation-contraction coupling (36). Excessive ROS generation in pathologic conditions such as ischemia/reperfusion (37), myocardial infarction (38), diabetic cardiomyopathy (37, 39), and liver disease (40), along with abnormal mitochondrial swelling and dysregulation of calcium buffering capacity, lead to mitochondrial disruption, and abnormal mitochondrial permeability which taken together trigger apoptotic signals and cell death (35). Uncoupling proteins are some of the mitochondrial parts which are negatively affected in the failing heart. They are physiologically involved in thermogenesis and energy expenditure (41), regulate mitochondrial membrane potential by proton translocation across the mitochondrial inner membrane, and effectively regulate ROS production (8). Indeed, these membrane proteins produce proton leak, so ROS generation is reduced following a decrease in the proton gradient across the mitochondrial inner membrane (8). It means that UCPs act as parts of the endogenous antioxidant defense system to protect ROS-induced mitochondrial damage (9).

Along with reducing the production of free radicals, they also reduce the production of adenosine triphosphate (ATP) by separating phosphorylation from oxidation, the phenomenon known as uncoupling (8). Some experimental studies indicate that cardiac UCP2 and UCP3 expression could negatively be influenced by several internal and/or external mediators such as irregular cellular redox status and excessive ROS generation during ischemia/reperfusion period, overproduction of inflammatory and pro-oxidant mediators as well as change in cellular energy consumption (8, 36, 42). According to previous studies, the UCP3-knockout rodent model exhibited a dramatic increase in ROS formation, diminished cardiac contractile performance, and increased mortality rate due to cardiac arrhythmia (42, 43). Both decrease (10) and increase (8) in the expression of cardiac UCP2 have been reported in different experimental models of ischemia and heart failure. Our findings revealed that a 4-week ligation of the bile duct could affect cardiac expression of mitochondrial UCP2 and UCP3. According to the physiologic role of cardiac UCPs, remarkable down-regulation of the cardiac genes could

result in increased ROS generation and consequently lead to oxidative stress-induced cardiac damage. On the other hand, mitochondrial ATP generation can increase following down-regulation of the UCPs. Considering the cardiac disability induced by a biliary obstruction, increased ATP production might be a compensatory mechanism to supply sufficient energy sources for counteracting impaired cardiac contractility.

Farnesoid X-activated receptors have a pivotal role in regulating the hemostasis of cellular redox status. Induction of some upstream and downstream signaling pathways such as activation of transcriptional factor Nrf2 and, consequently, increasing the formation of cellular GSH and SOD and several other endogenous antioxidants occurs following FXR activation (13-15). So, FXR activation protects against the deleterious effects of free radicals, which are over-produced in several pathological conditions (13, 16, 17). According to the previous studies, the cytoprotective and antioxidant activity of FXR is closely related to its regulatory effects on mitochondrial function (21). The findings of a study showed that long-term activation of FXR by a synthetic FXR agonist (GW4064) during the chronic phase of MI was associated with marked cardioprotective properties that inhibit cardiomyocyte apoptosis, suppressing inflammation and increasing the markers of angiogenesis and mitochondrial biogenesis (18). Gai *et al.* also reported that FXR activation in proximal tubular cells exposed to ischemic injury was accompanied with a clear reduction of mitochondrial damage and oxidative stress markers (13). Some findings indicate the protective role of FXR activation by either endogenous or exogenous ligands on liver disease via suppressing inflammation and fibrosis (44-47). There is, however, a discrepancy regarding the cardioprotective role of FXR during massive cardiac injury. In this regard, Qiang *et al.* reported that knocking out of FXR led to aggravation of cardiac cardiomyopathy and accumulation of excess fat, and development of fibrosis in the heart of diabetic mice (48). In agreement with the previous one, the cardioprotective role of FXR activation has been confirmed by others (18, 19).

In contrast, some reports indicate the deleterious effect of cardiac FXR activation following myocardial ischemia or infarction injury, including dissipation of mitochondrial membrane, mitochondrial dysfunction, and induction of apoptotic signals via mitochondrial-mediated cytochrome c-dependent caspase-9 activation pathway (20, 49, 50). So, despite the importance of FXR in cardiac function, there is still much uncertainty about their role in cardiac function during the development of massive cardiac disease. According to our results, induction of BDL for 4 weeks was associated with a significant reduction in the expression of both cardiac and hepatic FXR.

Given our microscopic findings, it is probable that FXR down-regulation is one of the critical elements involved in disease pathogenesis. Regarding the regulatory role of FXR on preserving antioxidant capacity, decreased FXR mRNA level can also impair its downstream pathways of Nrf2 and finally activation of glutathione related genes, so, involved organs are very vulnerable to deleterious effects of ROS generation. Impairment of antioxidant capacity and/or activity is also confirmed by down-regulating myocardial UCP2 and UCP3 expression. There is a direct relationship between cardiac FXR, UCP2, and UCP3 activity. Their down-regulation could finally impair both enzymatic (glutathione) and non-enzymatic (UCP's ROS buffering

capacity) antioxidant defense systems of the cardiomyocytes.

Conclusion

Considering the regulatory role of FXR and ROS buffering effects of mitochondrial UCPs, the observed reduction in the mRNA levels of targeted genes could be partially responsible for further exposure to deleterious damages of ROS generation. Taken together, FXR as upstream regulators of cellular redox status as well as cardiac UCPs have a pivotal role in the pathogenesis of cirrhotic-induced cardiac abnormality in rats.

Acknowledgment

The Laboratory technical assistance staff of the Paramedicine School of Alborz University of Medical Sciences are gratefully acknowledged. For this study, the authors received funding from the Vice Chancellor for Research, Alborz University of Medical Sciences, Karaj, Iran.

Conflicts of Interest

The authors state no conflicts of interest.

Authors' Contributions

GB, SAH, HK, PF, AKh, MB, and KH Helped with study conception and/or design; GB, AKh, HK, PF, KH, SAH, and MB Performed experiments, data collection analysis, and draft manuscript preparation; GB, HK, KH, MB, SAH, PF, and AKh Critically revised and/or edited the paper; AKh Supervised the research.

References

- Caramelo C Fau - Fernandez-Muñoz D, Fernandez-Muñoz D Fau - Santos JC, Santos Jc Fau - Blanchart A, Blanchart A Fau - Rodriguez-Puyol D, Rodriguez-Puyol D Fau - López-Novoa JM, López-Novoa Jm Fau - Hernando L, *et al.* Effect of volume expansion on hemodynamics, capillary permeability and renal function in conscious, cirrhotic rats. *Hepatology* 1986; 6:129-134.
- Cazzaniga M, Salerno F, Pagnozzi G, Dionigi E, Visentin S, Cirello I, *et al.* Diastolic dysfunction is associated with poor survival in patients with cirrhosis with transjugular intrahepatic portosystemic shunt. *Gut* 2007; 56:869-875.
- Carvalho MVH, Kroll PC, Kroll RTM, Carvalho VN. Cirrhotic cardiomyopathy: the liver affects the heart. *Braz J Med Biol Res* 2019; 52:e7809.
- Cichoż-Lach H, Michalak A. Oxidative stress as a crucial factor in liver diseases. *World J Gastroenterol* 2014; 20:8082-8091.
- Orr AL, Ashok D, Sarantos MR, Shi T, Hughes RE, Brand MD. Inhibitors of ROS production by the ubiquinone-binding site of mitochondrial complex I identified by chemical screening. *Free Radic Biol Med* 2013; 65:1047-1059.
- Meany DL, Poe BG, Navratil M, Moraes CT, Arriaga EA. Superoxide released into the mitochondrial matrix. *Free Radic Biol Med* 2006; 41:950-959.
- Mousavi K, Niknahad H, Ghalamfarsa A, Mohammadi H, Azarpira N, Ommati MM, *et al.* Taurine mitigates cirrhosis-associated heart injury through mitochondrial-dependent and antioxidative mechanisms. *Clin Exp Hepatol* 2020; 6:207-219.
- Safari F, Anvari Z, Moshtaghion S, Javan M, Bayat G, Forosh SS, *et al.* Differential expression of cardiac uncoupling proteins 2 and 3 in response to myocardial ischemia-reperfusion in rats. *Life Sci* 2014; 98:68-74.
- Chen GG, Yan JB, Wang XM, Zheng MZ, Jiang JP, Zhou XM, *et al.* Mechanism of uncoupling protein 2-mediated myocardial injury in hypothermic preserved rat hearts. *Mol Med Rep* 2016; 14:1857-1864.
- Bugger H, Guzman C, Zechner C, Palmeri M, Russell KS, Russell RR, 3rd. Uncoupling protein down-regulation in doxorubicin-induced heart failure improves mitochondrial coupling but increases reactive oxygen species generation. *Cancer Chemother Pharmacol* 2011; 67:1381-1388.
- Hoerter J, Gonzalez-Barroso MD, Couplan E, Mateo P, Gelly C, Cassard-Doulcier AM, *et al.* Mitochondrial uncoupling protein 1 expressed in the heart of transgenic mice protects against ischemic-reperfusion damage. *Circulation* 2004; 110:528-533.
- Teshima Y, Akao M, Jones Steven P, Marbán E. Uncoupling Protein-2 Overexpression Inhibits Mitochondrial Death Pathway in Cardiomyocytes. *Circ Res* 2003; 93:192-200.
- Gai Z, Chu L, Xu Z, Song X, Sun D, Kullak-Ublick GA. Farnesoid X receptor activation protects the kidney from ischemia-reperfusion damage. *Sci Rep* 2017; 7:9815.
- Haga S, Yimin, Ozaki M. Relevance of FXR-p62/SQSTM1 pathway for survival and protection of mouse hepatocytes and liver, especially with steatosis. *BMC Gastroenterol* 2017; 17:9-21.
- Zhang Y, Xu Y, Qi Y, Xu L, Song S, Yin L, *et al.* Protective effects of dioscin against doxorubicin-induced nephrotoxicity via adjusting FXR-mediated oxidative stress and inflammation. *Toxicology* 2017; 378:53-64.
- Gai Z, Gui T, Hiller C, Kullak-Ublick GA. Farnesoid X Receptor Protects against Kidney Injury in Uninephrectomized Obese Mice. *J Biol Chem* 2016; 291:2397-2411.
- Lu C, Zhang F, Xu W, Wu X, Lian N, Jin H, *et al.* Curcumin attenuates ethanol-induced hepatic steatosis through modulating Nrf2/FXR signaling in hepatocytes. *IUBMB Life* 2015; 67:645-658.
- Xia Y, Zhang F, Zhao S, Li Y, Chen X, Gao E, *et al.* Adiponectin determines farnesoid X receptor agonism-mediated cardioprotection against post-infarction remodeling and dysfunction. *Cardiovasc Res* 2018; 114:1335-1349.
- Wu H, Liu G, He Y, Da J, Xie B. Obeticholic acid protects against diabetic cardiomyopathy by activation of FXR/Nrf2 signaling in db/db mice. *Eur J Pharmacol* 2019; 858:172393.
- Gao J, Liu X, Wang B, Xu H, Xia Q, Lu T, *et al.* Farnesoid X receptor deletion improves cardiac function, structure and remodeling following myocardial infarction in mice. *Mol Med Rep* 2017; 16:673-679.
- Han CY, Kim TH, Koo JH, Kim SG. Farnesoid X receptor as a regulator of fuel consumption and mitochondrial function. *Arch Pharm Res* 2016; 39:1062-1074.
- Yang Y, Chen B, Chen Y, Zu B, Yi B, Lu K. A comparison of two common bile duct ligation methods to establish hepatopulmonary syndrome animal models. *Lab Anim* 2015; 49:71-79.
- Khalili A, Fallah P, Hashemi SA, Ahmadian-Attari MM, Jamshidi V, Mazloom R, *et al.* New mechanistic insights into hepatoprotective activity of milk thistle and chicory quantified extract: The role of hepatic Farnesoid-X activated receptors. *Avicenna J Phytomed* 2021; 11:367-379.
- Safari F, Hajiadeh S, Moshtaghion SH, Forouzandeh Moghadam M, Shekarforoush S, Bayat G, *et al.* Effect of losartan on NOX2 transcription following acute myocardial ischemia-reperfusion. *Physiol-Pharmacol* 2012; 16:44-53.
- Desai MS, Mathur B, Eblimit Z, Vasquez H, Taegtmeier H, Karpen SJ, *et al.* Bile acid excess induces cardiomyopathy and metabolic dysfunctions in the heart. *Hepatology* 2017; 65:189-201.
- Jazaeri F, Afsharmoghaddam R, Abdollahi A, Ghamami G, Dehpour AR. Evaluation of chronic losartan treatment effect on cardiac chronotropic dysfunction in biliary cirrhotic rats. *Acta Med Iran* 2018; 56:4-13.
- Cruz A, Tasset I, Ramírez LM, Arjona A, Segura J, Túnez I, *et al.* Effect of melatonin on myocardial oxidative stress induced by experimental obstructive jaundice. *Rev Esp Enferm Dig* 2009; 101:460-463.
- Matyas C, Erdelyi K, Trojnar E, Zhao S, Varga ZV, Paloczi J, *et*

- al. Interplay of Liver–Heart Inflammatory Axis and Cannabinoid 2 Receptor Signaling in an Experimental Model of Hepatic Cardiomyopathy. *Hepatology* 2020; 71:1391-1407.
29. Kemp R, Castro-e-Silva O, Santos JS, Sankarankutty AK, Correa RB, Baldo CF, *et al.* Evaluation of the mitochondrial respiration of cardiac myocytes in rats submitted to mechanical bile duct obstruction. *Acta Cir Bras* 2008; 23:66-71.
30. Lunseth JH, Olmstead EG, Abboud F. A study of heart disease in one hundred eight hospitalized patients dying with portal cirrhosis. *AMA Arch Intern Med* 1958; 102:405-413.
31. Chayanupatkul M, Liangpunsakul S. Cirrhotic cardiomyopathy: review of pathophysiology and treatment. *Hepatol Int* 2014; 8:308-315.
32. Sergeeva IA, Christoffels VM. Regulation of expression of atrial and brain natriuretic peptide, biomarkers for heart development and disease. *Biochim Biophys Acta* 2013; 1832:2403-2413.
33. Nunes S, Soares E, Fernandes J, Viana S, Carvalho E, Pereira FC, *et al.* Early cardiac changes in a rat model of prediabetes: brain natriuretic peptide overexpression seems to be the best marker. *Cardiovasc Diabetol* 2013; 12:44-54.
34. Januzzi JL, Jr. Natriuretic peptides as biomarkers in heart failure. *J Investig Med* 2013; 61:950-955.
35. Duran J, Martinez A, Adler E. Cardiovascular Manifestations of Mitochondrial Disease. *Biology (Basel)* 2019; 8:34-60.
36. Hilse KE, Rupprecht A, Egerbacher M, Bardakji S, Zimmermann L, Wulczyn AEMS, *et al.* The expression of uncoupling protein 3 coincides with the fatty acid oxidation type of metabolism in adult murine heart. *Front Physiol* 2018; 9:747.
37. Duncan JG. Mitochondrial dysfunction in diabetic cardiomyopathy. *Biochim Biophys Acta* 2011; 1813:1351-1359.
38. Ramachandra CJA, Hernandez-Resendiz S, Crespo-Avilan GE, Lin Y-H, Hausenloy DJ. Mitochondria in acute myocardial infarction and cardioprotection. *EBioMedicine* 2020; 57:102884.
39. Bugger H, Abel ED. Mitochondria in the diabetic heart. *Cardiovasc Res* 2010; 88:229-240.
40. Hassanein T. Mitochondrial dysfunction in liver disease and organ transplantation. *Mitochondrion* 2004; 4:609-620.
41. Viengchareun S, Penforis P, Zennaro M-C, Lombès M. Mineralocorticoid and glucocorticoid receptors inhibit UCP expression and function in brown adipocytes. *Am J Physiol Endocrinol Metab* 2001; 280:E640-E649.
42. Perrino C, Schiattarella GG, Sannino A, Pironti G, Petretta MP, Cannavo A, *et al.* Genetic deletion of uncoupling protein 3 exaggerates apoptotic cell death in the ischemic heart leading to heart failure. *J Am Heart Assoc* 2013; 2:e000086.
43. Harmancey R, Vasquez HG, Guthrie PH, Taegtmeier H. Decreased long-chain fatty acid oxidation impairs postischemic recovery of the insulin-resistant rat heart. *FASEB J* 2013; 27:3966-3978.
44. Verbeke L, Mannaerts I, Schierwagen R, Govaere O, Klein S, Vander Elst I, *et al.* FXR agonist obeticholic acid reduces hepatic inflammation and fibrosis in a rat model of toxic cirrhosis. *Sci Rep* 2016; 6-Last page.
45. Wu W, Zhu B, Peng X, Zhou M, Jia D, Gu J. Activation of farnesoid X receptor attenuates hepatic injury in a murine model of alcoholic liver disease. *Biochem Biophys Res Commun* 2014; 443:68-73.
46. Livero FA, Stolf AM, Dreifuss AA, Bastos-Pereira AL, Chicorski R, de Oliveira LG, *et al.* The FXR agonist 6ECDCA reduces hepatic steatosis and oxidative stress induced by ethanol and low-protein diet in mice. *Chem Biol Interact* 2014; 217:19-27.
47. Wang B, Zhang H, Luan Z, Xu H, Wei Y, Zhao X, *et al.* Farnesoid X receptor (FXR) activation induces the antioxidant protein metallothionein 1 expression in mouse liver. *Exp Cell Res* 2020; 390:111949.
48. Qiang S, Tao L, Zhou J, Wang Q, Wang K, Lu M, *et al.* Knockout of farnesoid X receptor aggravates process of diabetic cardiomyopathy. *Diabetes Res Clin Pract* 2020; 161:108033.
49. Pu J, Yuan A, Shan P, Gao E, Wang X, Wang Y, *et al.* Cardiomyocyte-expressed farnesoid-X-receptor is a novel apoptosis mediator and contributes to myocardial ischaemia/reperfusion injury. *Eur Heart J* 2013; 34:1834-1845.
50. Tsoporis James N, Izhar S, Desjardins Jean F, Salpeas V, Rizos Ioannis C, Parker Thomas G. Abstract 16846: Activation of farnesoid x receptor signaling mediates atrial myocyte apoptosis in patients undergoing on-pump coronary artery bypass grafting and ventricular remodeling after experimental myocardial infarction. *Circulation* 2017; 136:A16846-A16846.